

Structural Basis of Cleavage by RNase H of Hybrids of Arabinonucleic Acids and RNA^{†,‡}George Minasov,^{§,||} Marianna Teplova,^{§,||} Poul Nielsen,[⊥] Jesper Wengel,[#] and Martin Egli^{*,§}

Department of Molecular Pharmacology and Biological Chemistry and Drug Discovery Program, Northwestern University Medical School, Chicago, Illinois 60611-3008, Department of Chemistry, Odense University, University of Southern Denmark, DK-5230 Odense M, Denmark, and Department of Chemistry and Center for Synthetic Bioorganic Chemistry, University of Copenhagen, Universitetsparken 5, DK-2100 Copenhagen, Denmark

Received December 6, 1999

ABSTRACT: The origins of the substrate specificity of *Escherichia coli* RNase H1 (termed RNase H here), an enzyme that hydrolyzes the RNA strand of DNA–RNA hybrids, are not understood at present. Although the enzyme binds double-stranded RNA, no cleavage occurs with such duplexes [Lima, W. F., and Crooke, S. T. (1997) *Biochemistry* 36, 390]. Therefore, the hybrid substrates may not adopt a canonical A-form geometry. Furthermore, RNase H is exquisitely sensitive to chemical modification of the DNA strands in hybrid duplexes. This is particularly relevant to the RNase H-dependent pathway of antisense action. Thus, only very few of the modifications currently being evaluated as antisense therapeutics are tolerated by the enzyme, among them phosphorothioate DNA (PS-DNA). Recently, hybrids of RNA and arabinonucleic acid (ANA) as well as the 2′F-ANA analogue were shown to be substrates of RNase H [Damha, M. J., et al. (1998) *J. Am. Chem. Soc.* 120, 12976]. Using X-ray crystallography, we demonstrate here that ANA analogues, such as 2′F-ANA [Berger, I., et al. (1998) *Nucleic Acids Res.* 26, 2473] and [3.3.0]bicyclo-ANA (bc-ANA), may not be able to adopt sugar puckers that are compatible with pure A- or a B-form duplex geometries, but rather prefer the intermediate O4′-endo conformation. On the basis of the observed conformations of these ANA analogues in a DNA dodecamer duplex, we have modeled a duplex of an all-C3′-endo RNA strand and an all-O4′-endo 2′F-ANA strand. This duplex exhibits a minor groove width that is intermediate between that of A-form RNA and B-form DNA, a feature that may be exploited by the enzyme in differentiating between RNA duplexes and DNA–RNA hybrids. Therefore, the combination of the established structural and functional properties of ANA analogues helps settle existing controversies concerning the discrimination of substrates by RNase H. Knowledge of the structure of an analogue that exhibits enhanced RNA affinity while not interfering with RNase H activity may prove helpful in the design of future antisense modifications.

Second- and third-generation nucleic acid analogues are now emerging that have promising features for therapeutic antisense applications (1). Among the hundreds of nucleic acid modifications that were assessed over the past 10 years (2), several 2′-O-modified ribonucleic acid analogues display high affinities for RNA (3–6) and resistance to nucleases (7, 8). Both features are critical for the successful use of antisense compounds in vivo (9). In addition, the 2′-deoxy-2′-fluoro analogue of arabinonucleic acid (2′F-ANA, Figure 1) displays features that may warrant further exploration of its potential as an antisense oligonucleotide (AON) (10).

First, 2′F-ANA strands have enhanced RNA affinity relative to those of DNA and phosphorothioate DNA (PS-DNA, Figure 1). Second, 2′F-ANA–RNA hybrids are substrates of RNase H.

The capability of an AON to induce RNase H is an important consideration for judging its potential as an antisense therapeutic (ref 11 and cited literature). Stable pairing of AONs to target RNA was observed to lead to inhibition of gene expression via a steric block mechanism (12, 13). However, RNase H-mediated degradation of a target mRNA is a more common and well-documented mode of action with AONs (14). A mode of action that includes degradation of the target message may simply be more potent than one that is limited to interfering with splicing or the translational machinery. Thus, the target sites of AONs that do not activate RNase H are restricted to the 5′-untranslated region, the start codon and, splice sites within pre-mRNA (15). While many AONs display promising affinities for RNA (2, 9), only a handful form hybrids with RNA that are recognized and cleaved by RNase H. These include PS-DNA

[†] Supported by the Danish Natural Science Research Council (J.W.) and the NIH (Grant GM-55237 to M.E.).

[‡] Coordinates and structure factors have been deposited in the Nucleic Acid Database (entry code AD0008).

* To whom correspondence should be addressed. Phone: (312) 503-0845. Fax: (312) 503-0796. E-mail: m-egli@nwu.edu.

[§] Northwestern University Medical School.

^{||} These authors contributed equally to this work.

[⊥] University of Southern Denmark.

[#] University of Copenhagen.

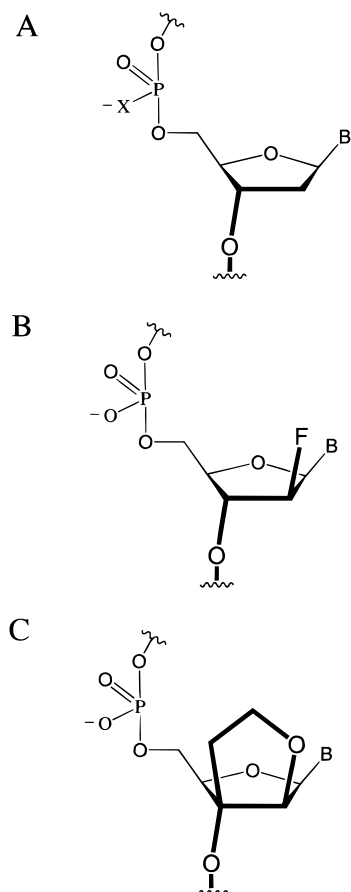


FIGURE 1: Structures of (A) DNA ($X = O$) and phosphorothioate DNA (PS-DNA, $X = S$), (B) 2'-deoxy-2'-fluoroarabinonucleic acid (2'F-ANA), and (C) [3.3.0]bicyclo-ANA (bc-ANA).

(16), phosphorodithioate DNA (17), and modifications affecting only the major groove such as C5-propynyl-modified pyrimidine and related modifications (ref 18 and cited literature).

Although RNase H binds to double-stranded DNA and RNA as well as to single-stranded nucleic acids and duplexes containing chemical modifications (other than those mentioned above), no cleavage was observed with such substrates (19). This is consistent with a recognition mechanism that includes probing the presence of 2'-hydroxyl groups in the minor groove as well as the overall conformational features of the substrate duplex. More specifically, the conformation of the DNA–RNA hybrid substrate recognized and processed by the enzyme may deviate from both the canonical A- and B-forms (20, 21). Oligodeoxynucleotides with incorporated 2'-O-modified nucleotides adopt standard A-type geometry (4), as do duplexes consisting of all-2'-O-modified strands (5). Therefore, the A-form geometry presumably adopted by duplexes of 2'-O-modified AONs and RNA precludes activation of RNase H and hydrolysis of the RNA strand.

In a B-DNA duplex, X-ray crystallographic data revealed strict adoption of an $O4'$ -endo sugar pucker by 2'F-ANA residues (22), consistent with the results of more recent MD simulations of the conformation of 2'F-ANA-containing duplexes (23). The $O4'$ -endo pucker (E) lies halfway between the $C2'$ -endo (S, B-DNA) and $C3'$ -endo (N, A-RNA) puckers (see Figure 2A for an illustration of sugar pucker ranges and terminology). Incorporation of 2'F-ANA residues into DNA leads to enhanced thermodynamic stability of the corre-

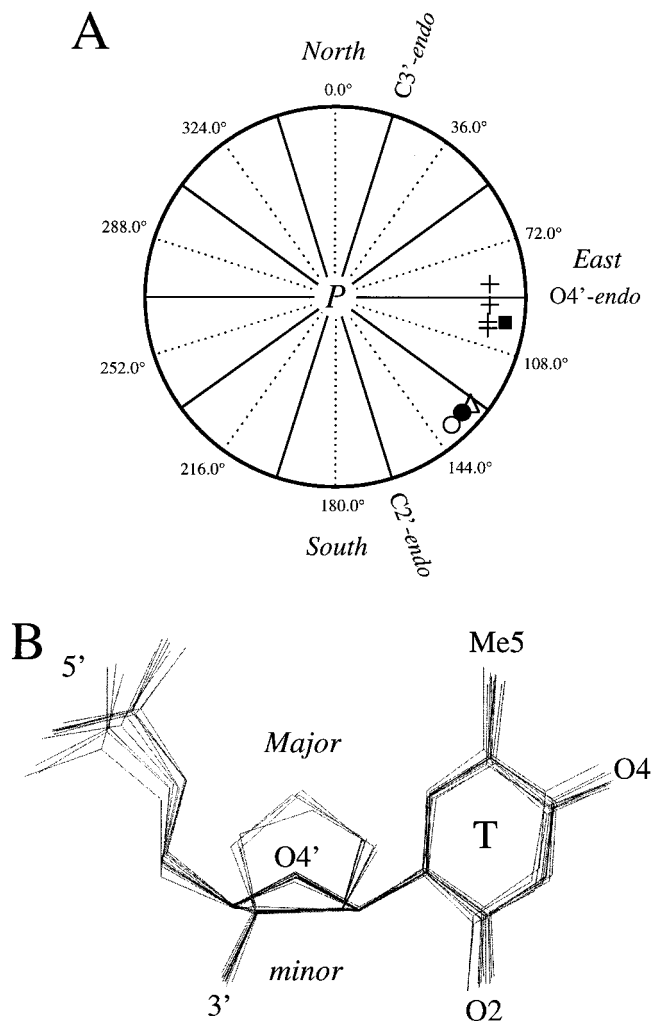


FIGURE 2: Conformations of 2'-O-modified arabinoses. (A) Schematic of the pseudorotation phase angle (P) cycle with the positions of selected pucker types indicated. The P angles of bc-ANA thymines in the BB duplex (+) are compared with the average P values of 2'F-ANA thymines in the FF and FT duplexes (■), 2'-deoxyriboses in the BB duplex (Δ ; terminal residues omitted), and the four thymines in the TT1 and TT2 duplexes (● and ○, respectively; see Table 2 for nomenclature). (B) Superposition of the sugar portions of the four bc-ANA thymines (BB duplex) and six 2'F-ANA thymines (FF and FT duplexes). The coordinates of 2'F-ANA residues were taken from the crystal structures of the FF and FT dodecamers published previously (22).

Table 1: Relative Thermodynamic Stabilities^a (Melting Temperatures ΔT_m) of bc-ANA- and 2'F-ANA-Modified Oligodeoxynucleotides Paired with Complementary RNA

AON sequence	ΔT_m (°C)	
	X = bc-ANA-T	X = 2'F-ANA-T
T ₅ X ₄ T ₅	+1	—
X ₁₃ T	+12.5	—
X ₁₈	—	+5
GXGAXXGC	-4	—
TTATATTTTTTCTTTCCC ^b	—	+14

^a Relative to DNA, compiled from refs 27 and 28 (bc-ANA) and 10 (2'F-ANA). ^b All 2'F-ANA.

sponding DNA duplexes relative to those of the native DNAs (22, 24–26) (Table 1). Two other ANA analogues, [3.3.0]-bicyclo-ANA (27, 28) (bc-ANA, Figure 1B) and [3.2.0]-bicyclo-ANA (29), were also found to exhibit enhanced affinity for RNA compared with that for DNA. Moreover,

Table 2: Sequences of the DNA Duplex with Incorporated bc-ANA Thymines and the 2'F-ANA-Modified and DNA Reference Duplexes

sequence	abbreviation	modification	resolution ^a (Å)	no. of reflections	ref
d(CGCGAA)–bc-ANA(TT)–d(CGCG)	BB	bc-ANA-T	1.43	12720	this paper
d(CGCGAA)–2'F-ANA(TT)–d(CGCG)	FF	2'F-ANA-T	1.65	7894	22
d(CGCGAA)–2'F-ANA(T)–d(TCGCG)	FT	2'F-ANA-T	1.60	8507	22
d(CGCGAATTTCGCG)	TT1	(adenosines cross-linked)	1.43	11200	49
d(CGCGAATTTCGCG)	TT2	wild type	1.40	11438	50

^a Taken from the original literature.

Table 3: Selected Crystal Data and Refinement Parameters for the BB Duplex

sequence	CGCGAA–bc-ANA(TT)–CGCG
crystal data	
space group	<i>P</i> 2 ₁ 2 ₁ 2 ₁
unit cell constants	
<i>a</i> (Å)	25.28
<i>b</i> (Å)	40.55
<i>c</i> (Å)	65.13
data collection	
X-ray source/detector	APS 5-ID/MARCCD
temperature (K)	105
total no. of reflections	115296
no. of unique reflections	13592
resolution (Å)	20–1.43
completeness (% , last shell)	99.9 (99.2)
<i>R</i> _{sym} ^a (% , last shell)	6.5 (18.8)
refinement statistics	
no. of DNA atoms	498
no. of waters	154
no. of Mg ²⁺ ions/spermines	1/1
rms distances (Å)	0.010
rms angles (deg)	1.55
no. of reflections (<i>F</i> > 0)	12720 (17–1.43 Å)
<i>R</i> -factor ^b (% , work set)	19.8
<i>R</i> -factor ^c (% , test set)	21.1

^a $R_{\text{sym}} = \sum_{hkl} \sum_i |I(hkl)_i - \langle I(hkl) \rangle| / \sum_{hkl} \sum_i \langle I(hkl)_i \rangle$. ^b $R\text{-factor} = \sum_{hkl} |F(hkl)_o - F(hkl)_c| / \sum_{hkl} F(hkl)_o$. ^c For 10% of the data.

the latter modification showed favorable pairing to DNA as well. Modeling studies were suggestive of the adoption of Eastern-type puckers by the bicyclic analogues (29). Both these results and those for 2'F-ANA may lead one to the fascinating conclusion that conformational restriction of an AON can lead to favorable duplex formation with DNA or RNA even if the preorganized conformation differs from those of the target strands (29).

MATERIALS AND METHODS

Oligonucleotide Synthesis and Crystallization. The BB dodecamer (see Table 2) was synthesized by the phosphoramidite method on a 2.5 μmol scale using published protocols for the synthesis of the bc-ANA-T building block (27, 28). The DMT-on oligonucleotide was purified by RP-HPLC (C4 column, TEAA buffer, pH 7.0, acetonitrile eluent), and after deprotection, the DMT-off material was HPLC-purified a second time. The dodecamer was crystallized by the hanging drop vapor diffusion method, equilibrating a 4 μL droplet [1 mM 12mer, 25 mM sodium cacodylate (pH 6.8), 25 mM Mg(OAc)₂, and 3 mM spermine] against a reservoir of 1 mL of 35% MPD. Selected crystal data are listed in Table 3.

X-ray Data Collection, Data Processing, and Structure Determination. A crystal was mounted in a nylon loop and flash-frozen in a nitrogen stream (105 K). High- and low-resolution data sets were collected on the 5-ID beamline ($\lambda = 1.0000$ Å) of the DND-CAT at the Advanced Photon

Source (Argonne, IL) using a MARCCD detector. Data were integrated and merged in the DENZO/SCALEPACK suite (30) ($R_{\text{merge}} = 6.5\%$) and are 100% complete to 1.43 Å (Table 3). The crystal structure of the FT dodecamer duplex with nucleic acid database (NDB) code BD0007 served as the initial model for refinement with the program CNS (31). Residues T7 and T8 in one strand and T19 and T20 in the opposite one were omitted, and the bc-ANA thymines were built into $F_o - F_c$ Fourier difference electron density maps. All data (12 720 reflections with $F > 0$) were used in the final refinement cycles. Final *R*-factors and rms deviations of the model from standard values for DNA bonds and angles are listed in Table 3, and examples of the quality of the final electron density are depicted in panels A and B of Figure 3.

Construction of a 2'F-ANA–RNA Hybrid Duplex. Because fully 2'F-ANA-modified oligo(T) strands were used for conducting both UV melting experiments (T₁₃, Table 1) and RNase H-mediated cleavage assays of duplexes (T₁₈; 10), we decided to model a duplex with 2'F-ANA thymines in one strand and 2'-riboadenosines in the complementary one. The puckers of arabinoses are of the O4'-endo type and based on the conformation of the bc-ANA(T7pT8) dimer in the crystal structure of the BB dodecamer. The puckers of riboses are of the C3'-endo type, consistent with the conformational preferences of the sugar moiety in canonical RNA duplexes. To construct the hybrid duplex, an r(AA)–r(UU) dimer duplex was created in TURBO-FRODO (32) such that the two pyrimidine bases could be perfectly superimposed on the bases and glycosyl bonds of the bc-ANA(T7pT8) dimer. Then the helical parameters of the bc-ANA(TT)–r(AA) miniduplex were calculated with the program CURVES (33), and on the basis of these parameters, a hybrid bc-ANA(T)₁₂–r(A)₁₂ duplex was generated. To obtain a uniform conformation of arabinoses in the bc-ANA strand, the sugar moieties of the six T7 residues in the duplex model were replaced by the arabinose of a T8 residue (the *P* angles of T7 and T8 differ by 16°; Table 4). Because it is currently not known whether bc-ANA–RNA hybrids generally are substrates of RNase H, we replaced the bc-ANA ethoxy bridges with 2'-fluorine atoms in the final model (Figure 4). Concerning the question of whether bc-ANA–RNA hybrids are substrates of RNase H, it is worth noting that the bc-ANA(T₁₃)d(T)–r(A)₁₄ duplex has been shown not to activate RNase H (H. Brummel and M. H. Caruthers, unpublished data).

RESULTS AND DISCUSSION

Crystal Structure of a DNA Dodecamer Duplex with bc-ANA-T Modifications. To analyze the conformational properties of bc-ANA residues, we synthesized the DNA dodecamer CGCGAA–bc-ANA(TT)–CGCG with two incorporated bc-ANA thymines (BB dodecamer, Table 2), crystallized it, and determined the crystal structure at 1.43 Å resolution. The

Table 4: Sugar Conformations and Pseudorotation Phase Angles P in the bc-ANA-Modified Duplex^a

strand 1/2 residue	P (deg)	pucker type
C 1/13	164/166	C2'-endo/C2'-endo
G 2/14	158/141	C2'-endo/C1'-exo
C 3/15	44/42	C4'-exo/C4'-exo
G 4/16	164/170	C2'-endo/C2'-endo
A 5/17	153/172	C2'-endo/C2'-endo
A 6/18	151/136	C2'-endo/C1'-exo
T 7/19 ^b	85/99	O4'-endo/O4'-endo
T 8/20 ^b	101/93	O4'-endo/O4'-endo
C 9/21	156/148	C2'-endo/C2'-endo
G 10/22	144/146	C1'-exo/C2'-endo
C 11/23	164/21	C2'-endo/C3'-endo
G 12/24	138/12	C1'-exo/C3'-endo

^a Calculated with the program CURVES (33). ^b bc-ANA-T.

dodecamer adopts an overall B-form geometry with the majority of the deoxyriboses adopting puckers in the Southern conformational range (C2'-endo and C1'-exo, Table 4 and Figure 2A). However, the four modified ANA residues display sugar puckers that fall uniformly within the O4'-endo range. The average pseudorotation phase angle P for bc-ANA sugars is 94° with a standard deviation of ±6°.

The preferred geometry of bc-ANA thymines observed here is very similar to that found for 2'F-ANA thymines in previously determined crystal structures of the FT and FF dodecamer duplexes (Table 2 and Figure 2) (22). The average P angle for 2'F-ANA residues in those duplexes was 99° with a standard deviation of ±3°. Thus, it appears that the sugar moieties of certain conformationally restricted arabinotype AONs show a specific preference for the O4'-endo conformational range. Detailed inspection of the backbone geometry and close contacts in the region of the bc-ANA modifications reveal that several 1–5-type interactions render impossible large variations in the geometry of bc-ANA residues within a B-form duplex (Figure 3). Steric constraints within the bicyclic ANA framework alone prohibit adoption of either the C2'-endo or C3'-endo pucker mode. Although the steric and stereoelectronic contributions to this conformational preference most certainly differ for 2'F-ANA and bc-ANA, both display enhanced RNA affinity relative to that for DNA as shown in Table 1 (10, 27, 28).

In terms of both sugar conformation and RNA affinity, 2'F-ANA and bc-ANA differ considerably from ANA itself (2'-OH). Computational simulations showed that ANA sugars prefer the C2'-endo pucker due to an intranucleoside O2'-H...O5' hydrogen bond (23). Crystal structures of Z-DNA duplexes that contain ANA residues confirm this preference for the Southern conformational range (34, 35). Further, ANA-RNA duplexes are less stable thermodynamically than the corresponding DNA-RNA hybrids (10). The relative order of stability of hybrid duplexes with RNA is as follows: 2'F-ANA > DNA > PS-DNA > ANA.

Geometry of the Duplex Recognized by RNase H. 2'F-ANA-RNA hybrids are better substrates for RNase H than ANA-RNA hybrids (10). This could partly be related to the relative thermal stabilities of these duplexes, but the observation may also hint at a correlation between the conformation of the DNA strand and the efficiency with which RNase H can cleave the RNA complement. X-ray crystal structures of DNA duplexes with at least one RNA residue per strand (36–40) and DNA-RNA hybrids (41–

44) all reveal a geometry that is close to the A-form and sugars with C3'-endo pucker. However, NMR solution data for DNA-RNA hybrids furnished a different result; the RNA strand adopted an A-type geometry, whereas the geometry of the DNA strand seemed to share features of both the A- and B-form (ref 21 and cited literature). The precise conformation adopted by the deoxyriboses was somewhat controversial. Both possibilities, a 1:1 mixture of the C2'-endo and C3'-endo modes as well as a more Eastern sugar geometry, were proposed (ref 45 and cited literature).

We have constructed a duplex that features an (A)₁₂ RNA strand with an A-type geometry (C3'-endo sugars, uniform $P = 13^\circ$) paired to a (T)₁₂ strand that is based on the geometry of the bc-ANA(T7pT8) dimer in the BB duplex crystal structure (O4'-endo sugars, uniform $P = 100^\circ$) (Figure 4; for details, see Materials and Methods). Its helical rise is 2.7 Å with a helical twist of 30.5°, and the overall geometry closely resembles that of a nonamer DNA-RNA duplex based on NMR solution experiments (21) (Figure 4C). The minor groove width of the duplex is 9.0 Å and thus narrower than the corresponding groove in A-RNA or in RNA-DNA duplexes (Table 5). Taken together, the X-ray crystallographic results demonstrate that bc-ANA and 2'F-ANA residues adopt similar Eastern-type puckers. Moreover, an oligonucleotide with a nearly ideal E-pucker sugar-phosphate backbone can be paired with an A-type RNA strand, and the resulting duplex adopts neither A- nor B-form geometry.

A minor groove width that is intermediate between those of pure A- and B-form duplexes is believed to be an important factor in the mechanism that allows RNase H to discriminate between DNA-RNA and RNA-RNA species (21). Because 2'F-ANA-RNA hybrids are substrates for RNase H and a 2'F-ANA strand cannot adopt a canonical B-form geometry or a conformation that results from a mixture of C2'-endo and C3'-endo sugar geometries, we conclude that the geometries of deoxyriboses in DNA-RNA hybrids that are processed by RNase H fall within the O4'-endo range (or within the neighboring 36° P ranges). This is consistent with NMR solution data (21) and provides evidence that does not support a mixture of C2'-endo and C3'-endo puckers in the DNA strand of the hybrid duplex.

It is now clear that DNA-RNA hybrids can adopt a variety of conformations. The actual conformation depends on the environment (crystal, solution, enzyme active site, etc.), sequence, ionic strength, hydration, and other factors. Thus, the hybrid duplex may adopt a canonical A-form geometry, or alternatively, at the other end of the conformational spectrum, feature an all-C3'-endo RNA strand paired with an all-C2'-endo DNA strand. However, the conformational dominance by the RNA portion in DNA-RNA hybrids as suggested by X-ray crystallographic data is unlikely to be representative of the situation at the active site of the RNase H enzyme (though it may well be the conformation adopted by the DNA-RNA complex at the active site of reverse transcriptases; see ref 46). Although the interactions between RNase H and the DNA-RNA hybrid substrate were modeled on the basis of the crystal structure of the enzyme and NMR solution structures of DNA-RNA hybrids (21) and a chemically modified substrate (47), no crystal structure of the enzyme-substrate complex has been reported to date. Therefore, definitive confirmation of the predicted conformation of the substrate

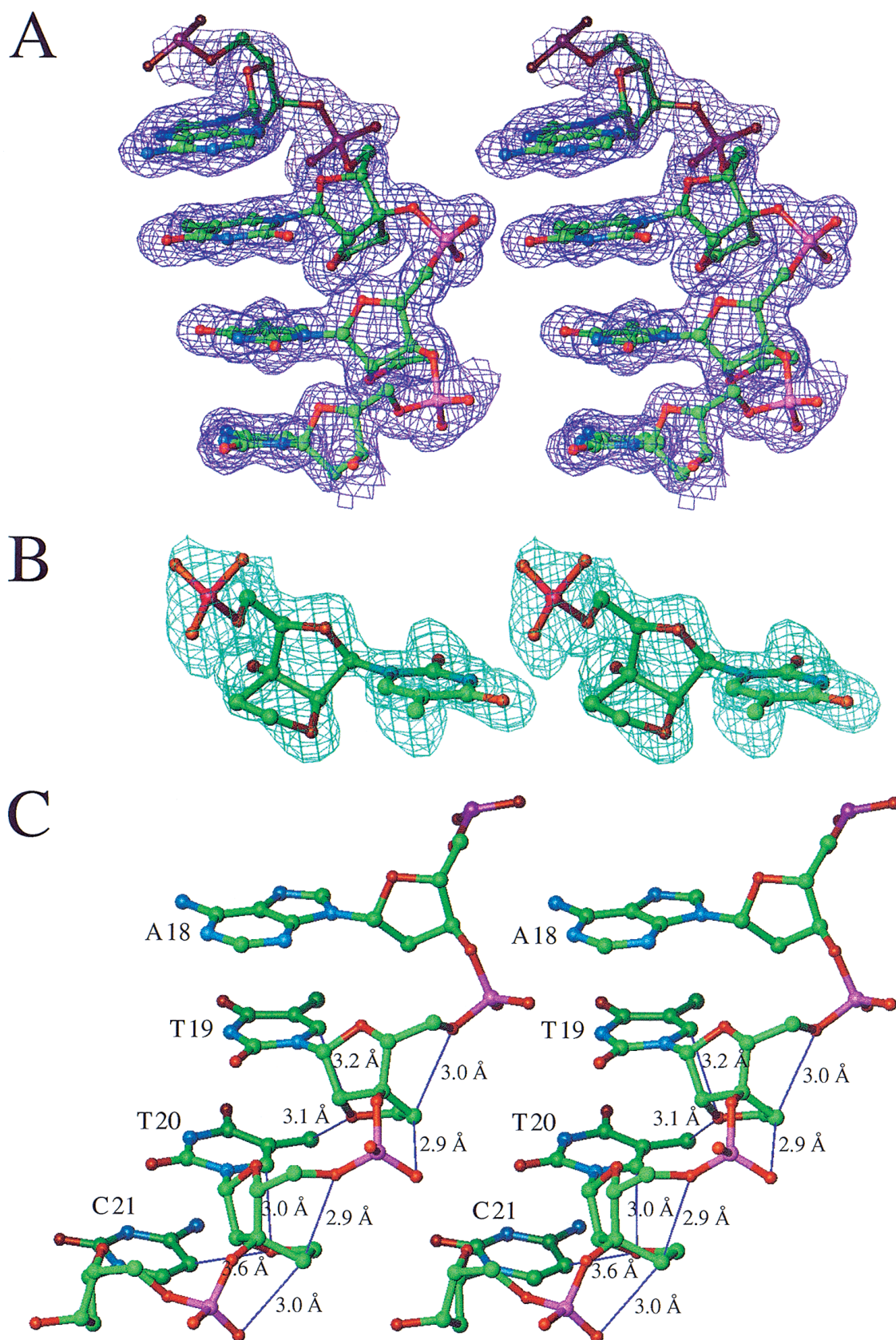


FIGURE 3: (A) Quality of the BB duplex structure. Stereodigram of the $2F_o - F_c$ Fourier sum electron density (1 σ level) surrounding nucleotides A18, bc-ANA-T19, and bc-ANA-T20 and C21. (B) Simulated annealing (SA) omit electron density (2 σ level) around nucleotide bc-ANA-T8. To generate the electron density map, the 2'-oxygen and the carbon atoms of the adjacent ethylene bridge from all four bc-ANA residues were omitted together with atoms located within spheres with 3 Å radii around the former (14% of all atoms in the asymmetric unit). This partial model was subjected to simulated annealing (31). (C) Stereodigram of the conformation of the tetramer fragment dA18-bc-ANA(T19pT20)-dC21 in the crystal structure of the BB duplex. Key contacts are depicted as thin lines with distances in angstroms. DNA atoms are colored green, red, cyan, and magenta for carbon, oxygen, nitrogen, and phosphorus, respectively.

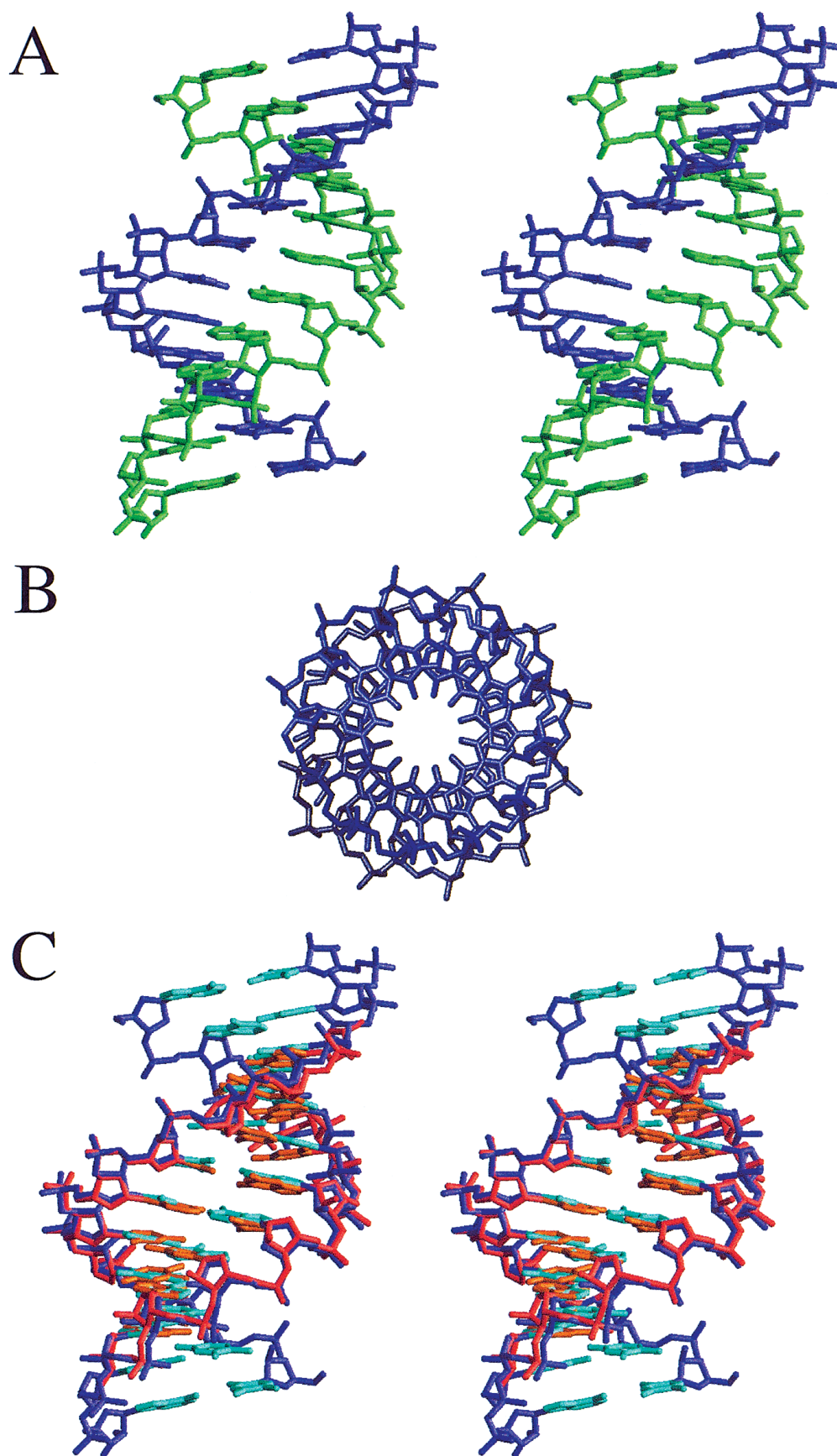


FIGURE 4: Geometry of the modeled 2'F-ANA(T)₁₂-r(A)₁₂ duplex. (A) Stereodigram of the duplex viewed down the minor groove. The 2'F-ANA oligo(T) strand is colored blue, and the RNA oligo(A) strand is colored green. (B) The duplex viewed along the helical axis, showing the axial displacement of bases. (C) Stereodigram depicting a superposition of the 2'F-ANA(T)₁₂-r(A)₁₂ duplex and the DNA-RNA hybrid duplex r(CAUGUGAC)-d(GTCACATG) whose structure had been determined by solution NMR (21). The sugar-phosphate backbones and bases of the 2'F-ANA(T)₁₂ and r(A)₁₂ strands in the 2'F-ANA-RNA duplex are colored blue and cyan, respectively. The sugar-phosphate backbones and bases of the DNA and RNA strands in the DNA-RNA duplex are colored red and orange, respectively.

Table 5: Minor and Major Groove Widths of Various Nucleic Acid Duplexes^a

duplex model	sequence	minor groove width ^b (Å)	major groove width ^b (Å)	ref
Figure 4 model	2'F-ANA(T) ₁₂ /r(A) ₁₂	9.0	8.2	this paper
RNA-DNA chimera	r(G)d(CGTATACGC)	9.8 (1.1)	3.6 (0.2)	38
RNA-DNA chimera	r(GCAGUGGC)-r(GCCA)d(CTGC)	10.1 (0.5)	8.2 (0.5)	40
RNA-DNA hybrid	r(UUCGGGCGCC)-d(GGCGCCCGAA)	9.6 (0.8)	5.3 (0.4)	41
RNA-DNA hybrid	r(GAAGAAGAA)-d(TTCTTCTTC)	9.7 (0.5)	8.2 (1.0)	42
RNA-DNA hybrid	r(GAAGAGAAGC)-d(GCTTCTCTTC)	9.8 (0.5)	8.5 (0.6)	43
RNA-DNA hybrid	r(CAUGUGAC)-d(GTCACATG)	8.8	7.9	21
A-RNA	r(CCCCGGGG)	9.8	6.9	51
B-DNA	fiber	5.7	11.7	52

^a Based on P...P distances minus 5.8 Å. ^b Standard deviations in parentheses.

at the enzyme active site has to await the experimental high-resolution structure of the complex of the enzyme and a DNA-RNA hybrid substrate.

CONCLUSIONS

Structural studies of conformationally restricted nucleic acid analogues such as the modified ANAs described here in combination with functional and thermodynamic stability data (10) allow refined interpretation of the specificity of RNase H. In particular, the 2'F-ANA modification appears to mimic the conformation adopted by the DNA strand in DNA-RNA hybrids which are substrates of this enzyme. An assessment of the processing of polypurine-RNA primer-2'F-ANA hybrids by the RNase H portion of reverse transcriptases may furnish insight into the role of the substrate conformation in protecting the primer-DNA complex against degradation (48). The standard A-form geometry (not possible with the 2'F-ANA-RNA hybrid) presumably adopted by this region is believed to inhibit the enzyme (42). In terms of therapeutic antisense applications, it remains to be seen whether there are alternative ANA modifications that will exhibit enhanced RNA affinity relative to 2'F-ANA while still activating RNase H.

ACKNOWLEDGMENT

We thank Ms. Britta M. Dahl for oligonucleotide synthesis. The DuPont-Northwestern-Dow Collaborative Access Team Synchrotron Research Center at the Advanced Photon Source is supported by E. I. DuPont de Nemours & Co., The Dow Chemical Co., the NSF, and the State of Illinois.

REFERENCES

- Crooke, S. T. (1998) in *Handbook of experimental pharmacology, Vol. 131, Antisense Research and Applications* (Crooke, S. T., Ed.) pp 1-50, Springer-Verlag, Berlin and Heidelberg, Germany.
- Freier, S. M., and Altmann, K.-H. (1997) *Nucleic Acids Res.* 25, 4429-4443.
- Altmann, K.-H., Fabbro, D., Dean, N. M., Geiger, T., Monia, B. P., Müller, M., and Nicklin, P. (1996) *Biochem. Soc. Trans.* 24, 630-637.
- Tereshko, V., Portmann, S., Tay, E. C., Martin, P., Natt, F., Altmann, K.-H., and Egli, M. (1998) *Biochemistry* 37, 10626-10634.
- Teplova, M., Minasov, G., Tereshko, V., Inamati, G. B., Cook, P. D., Manoharan, M., and Egli, M. (1999) *Nat. Struct. Biol.* 6, 535-539.
- Wengel, J. (1999) *Acc. Chem. Res.* 32, 301-310.
- Griffey, R. H., Monia, B. P., Cummins, L. L., Freier, S. M., Greig, M. J., Guinosso, C. J., Lesnik, E., Manalili, S. M., Mohan, V., Owens, S. R., Ross, B. R., Sasmor, H., Wanczewicz, E., Weiler, K., Wheeler, P. D., and Cook, P. D. (1996) *J. Med. Chem.* 39, 5100-5109.
- Teplova, M., Wallace, S. T., Minasov, G., Tereshko, V., Symons, A., Cook, P. D., Manoharan, M., and Egli, M. (1999) *Proc. Natl. Acad. Sci. U.S.A.* 96, 14240-14245.
- Cook, P. D. (1998) *Annu. Med. Rep. Chem.* 33, 313-325.
- Damha, M. J., Wilds, C. J., Noronha, A., Brukner, I., Borkow, G., Arion, D., and Parniak, M. A. (1998) *J. Am. Chem. Soc.* 120, 12976-12977.
- Crooke, S. T., Lemonidis, K. M., Neilson, L., Griffey, R., Lesnik, E. A., and Monia, B. P. (1995) *Biochem. J.* 312, 599-608.
- Baker, B. F., Lot, S. S., Condon, T. P., Cheng-Flourney, S., Lesnik, E. A., Sasmor, H. M., and Bennett, C. F. (1997) *J. Biol. Chem.* 272, 11994-12000.
- Heidenreich, O., Gryaznov, S., and Nerenberg, M. (1997) *Nucleic Acids Res.* 25, 776-780.
- Crooke, S. T. (1993) *Antisense Nucleic Acid Drug Dev.* 8, 133-134.
- Taylor, M. F., Widerholt, K., and Sverdrup, F. (1999) *Drug Discovery Today* 4, 562-567.
- Eckstein, F. (1986) *Annu. Rev. Biochem.* 54, 367-402.
- Marshall, W. S., and Caruthers, M. H. (1993) *Science* 259, 1564-1570.
- Flanagan, W. M., Wolf, J. J., Olson, P., Grant, D., Lin, K.-Y., Wagner, R. W., and Matteucci, M. D. (1999) *Proc. Natl. Acad. Sci. U.S.A.* 96, 3513-3518.
- Lima, W. F., and Crooke, S. T. (1997) *Biochemistry* 36, 390-398.
- Salazar, M., Champoux, J. J., and Reid, B. R. (1993) *Biochemistry* 32, 739-744.
- Fedoroff, O. Y., Salazar, M., and Reid, B. R. (1993) *J. Mol. Biol.* 233, 509-523.
- Berger, I., Tereshko, V., Ikeda, H., Marquez, V. E., and Egli, M. (1998) *Nucleic Acids Res.* 26, 2473-2480.
- Venkateswarlu, D., and Ferguson, D. M. (1999) *J. Am. Chem. Soc.* 121, 3009-3010.
- Rosenberg, I., Farras Soler, J., Tocik, Z., Ren, W.-Y., Ciszewski, L. A., Kois, P., Pankiewicz, K. W., Spassova, M., and Watanabe, K. A. (1993) *Nucleosides Nucleotides* 12, 381-401.
- Kois, P., Tocik, Z., Spassova, M., Ren, W.-Y., Rosenberg, I., Farras Soler, J., and Watanabe, K. A. (1993) *Nucleosides Nucleotides* 12, 1093-1109.
- Ikeda, H., Fernandez, R., Wilk, A., Barchi, J. J., Huang, X. L., and Marquez, V. E. (1998) *Nucleic Acids Res.* 26, 2237-2244.
- Nielsen, P., Pfundheller, H. M., and Wengel, J. (1997) *Chem. Commun.* 9, 825-826.
- Nielsen, P., Pfundheller, H. M., Olsen, C. E., and Wengel, J. (1997) *J. Chem. Soc., Perkin Trans. 1*, 3423-3433.
- Christensen, N. K., Petersen, M., Nielsen, P., Jacobsen, J. P., Olsen, C. E., and Wengel, J. (1998) *J. Am. Chem. Soc.* 120, 5458-5463.
- Otwinowski, Z., and Minor, W. (1997) *Methods Enzymol.* 276, 307-326.
- Brünger, A. T. (1998) *Crystallography & NMR System (CNS)*, version 0.4, Yale University, New Haven, CT.

32. Cambillau, C., and Roussel, A. (1997) TURBO-FRODO, version OpenGL.1, Université Aix-Marseille II, Marseille, France.
33. Lavery, R., and Sklenar, H. (1989) *J. Biomol. Struct. Dyn.* 6, 655–667.
34. Teng, M.-K., Liaw, Y.-C., van der Marel, G. A., van Boom, J. H., and Wang, A. H.-J. (1989) *Biochemistry* 28, 4923–4928.
35. Zhang, H., van der Marel, G. A., van Boom, J. H., and Wang, A. H.-J. (1992) *Biopolymers* 32, 1559–1569.
36. Wang, A. H.-J., Fujii, S., van Boom, J. H., van der Marel, G. A., van Boeckel, S. A. A., and Rich, A. (1980) *Nature* 299, 601–604.
37. Egli, M., Usman, N., Zhang, S., and Rich, A. (1992) *Proc. Natl. Acad. Sci. U.S.A.* 89, 534–538.
38. Egli, M., Usman, N., and Rich, A. (1993) *Biochemistry* 32, 3221–3237.
39. Ban, C., Ramakrishnan, B., and Sundaralingam, M. (1994) *J. Mol. Biol.* 236, 275–285.
40. Müller, U., Maier, G., Onori Mochi, A., Cellai, L., Heumann, H., and Heinemann, U. (1998) *Biochemistry* 37, 12005–12011.
41. Horton, N. C., and Finzel, B. C. (1996) *J. Mol. Biol.* 264, 521–533.
42. Xiong, Y., and Sundaralingam, M. (1998) *Structure* 6, 1493–1501.
43. Conn, G., Brown, T., and Leonard, G. A. (1999) *Nucleic Acids Res.* 27, 555–561.
44. Pley, H. W., Flaherty, K. M., and McKay, D. B. (1994) *Nature* 372, 68–74.
45. Cheatham, T. E., III, and Kollman, P. A. (1997) *J. Am. Chem. Soc.* 119, 4805–4825.
46. Huang, H., Chopra, R., Verdine, G. L., and Harrison, S. C. (1998) *Science* 282, 1669–1675.
47. Nakamura, H., Oda, Y., Iwai, S., Inoue, H., Ohtsuka, E., Kanaya, S., Kimura, S., Katsuda, C., Katayanagi, K., Morikawa, K., Miyashiro, H., and Ikehara, M. (1991) *Proc. Natl. Acad. Sci. U.S.A.* 88, 11535–11539.
48. Coffin, J. M. (1996) in *Virology* (Fields, B. N., and Straus, S. E., Eds.) 3rd ed., pp 1767–1847, Lippincott-Raven Publishers, New York.
49. Chiu, T. K., Kaczor-Grzeskowiak, M., and Dickerson, R. E. (1999) *J. Mol. Biol.* 292, 589–608.
50. Shui, X., McFail-Isom, L., Hu, G. H., and Williams, L. D. (1998) *Biochemistry* 37, 8341–8355.
51. Egli, M., Portmann, S., and Usman, N. (1996) *Biochemistry* 35, 8489–8494.
52. Saenger, W. (1984) *Principles of Nucleic Acid Structure*, Springer-Verlag, New York.

BI992792J